ICUC9 - 9th International Conference on Urban Climate jointly with 12th Symposium on the Urban Environment

Urban Canopy Air Quality and Breathability

Negin Nazarian[a,1,*], Alberto Martilli[b], Jan Kleissl[a]

[a] *Mechanical and Aerospace Engineering, University of California San Diego, La Jolla, CA*

[b] *Center for Energy, Environment and Technology (CIEMAT), Madrid, Spain*

1. Introduction

As urbanization progresses, more comprehensive and advanced methods are required to analyze the modifications of urban microclimate. Among various factors that alter urban environments from undisturbed climates, street level air pollution due to vehicular exhausts is of major concern and is significantly affected by atmospheric motion and stability. Thermal forcing is shown to play an important role in determining flow patterns and pollutant dispersion in built environments [1, 2], yet numerical studies of dispersion at microscale in urban areas are limited to simplified and uniform thermal conditions and the analyses on the effect of realistic surface heating are scarce.

To address this shortcoming, a detailed indoor-outdoor building energy model (TUF-IOBES) is employed to compute heat fluxes from street and building surfaces, which are then used as boundary condition for a PArallelized Large-Eddy Simulation Model (PALM). In comparison with previous studies, our model considers the transient non-uniform surface heating caused by solar insolation and inter-building shadowing, while coupling the indoor-outdoor heat transfer, flow field and passive pollution dispersion. Series of fluid flow and thermal field simulations are then performed for an idealized, compact mid-rise urban environment with no vegetation and the pollution dispersion and exchange behavior in and above buildings is investigated.

The following sections describe the methodology and structure of the presented work. Numerical tools and the simulation setup are described in Section 2. The characterization of the flow and thermal field is examined and their degree of universality is evaluated in section 3 as a function of two dimensionless number. Subsequently, spatial distribution of dimensionless concentration and turbulent fluxes are investigated as varied with the prescribed characterization method in Section 4. Additionally, street canyon pollutant exchange performance, i.e removal of the ground level traffic emissions from the top and lateral ventilating faces of the building canyon is examined by means of Air Exchange Rate (ACH) in Section 4.2.

2. Methods and simulation setup

Large Eddy Simulations are used as a superior method for evaluating turbulence characteristics and dispersion behavior in the street canyon. The PArallelized Large-eddy simulation Model (PALM) developed at the Leibniz University of Hannover (Raasch et al. [3] and Letzel et al. [4]) is employed with realistic thermal boundary conditions extracted from Temperature of Urban Facets Indoor-Outdoor Building Energy Simulation [5]. TUF-IOBES as well as the velocity and temperature fields of PALM were validated by Yaghoobian and Kleissl [5] and Park et al. [6] respectively. Yaghoobian et al. [7] validated the coupling method against the wind-tunnel experiment of Kovar-Panskus et al. [8] and demonstrated that one-way coupling of TUF-IOBES surface heat flux to PALM can account for the effects of the realistic temperature distribution over urban canopy surfaces. For the purpose of this study, the prognostic equation for passive scalars is also solved in PALM that was validated in Park et al. [6].

All simulations are performed over an array of uniformly spaced obstacles with a canyon aspect ratio (canyon height-to-width) of 1 and the configuration represents compact low rise urban zone, corresponding to a roughness plan aspect ratio, $\lambda_p = A_p/A_T$, of 0.29 and frontal aspect ratio, $\lambda_f = A_f/A_T$, of 0.25. A_p , A_f and A_T

*Corresponding author, Tel.: +1 8586999870

Email addresses: nenazarian@ucsd.edu (Negin Nazarian), alberto.martilli@ciemat.es (Alberto Martilli), jkleissl@ucsd.edu (Jan Kleissl)

Table 1: surface radiative and material properties

Surface	Roof	Ground	Walls
Albedo (-)	0.6	0.1	0.3
Emissivity (-)	0.9	0.95	0.9
Roughness length (m)	0.0005	0.0005	0.0005

indicate the plan area, the frontal area and the total area of roughness elements, respectively. Total domain height is 7.4H, where H is the building height. Each building wall has a window fraction of 0.47.
Thermal, radiative and material properties of urban surfaces are shown in Table 1. Latent heat fluxes are assumed to be zero. There is a window considered on all walls and the windows heat flux is computed based on the ASHRAE Toolkit. Surface heat flux at each grid points from TUF-IOBES are outputted in 15 minutes intervals and temporally interpolated to PALM. Periodic boundary conditions are used in horizontal directions, conserving mass-flow rate in the streamwise direction. Uniform and constant pollutant emission is prescribed at the ground boundary condition (z=0), representing traffic emission. A constant sink term for scalar flux is imposed as top boundary condition. Using this boundary condition, the integral of the concentration in the whole domain is constant in time, therefore, the ensemble average can be approximated by the time average. Additionally, above the buildings the turbulent flux is nearly constant with height, which is a typical feature for the inertial sublayer (e.g. the upper part of the atmospheric surface layer).
LES explicitly resolves turbulence and simulates one realization of the flow. Results must be time averaged to obtain statistically significant quantities. The definition of the averaging interval is crucial. A guiding principle is that, given the regularity of the array and the periodic boundary conditions, the time averaged flow in all the canyons must be identical. However, 30 min averaged velocity fields shows a strong variability between different canyons. This behavior is due to the formation of roll-like circulations with axes in streamwise direction. Coceal et al. [9] with DNS showed that to filter these it is necessary to average over at least 400 large eddy turnovers, that for our set-up, corresponds to about 11 hours. They also observed that the so-called dispersive stress (Raupach and Shaw [10] becomes zero above the canopy when the time averaging is large enough. In our case, however, it is not possible to use 11 h as averaging time, since the heat fluxes change significantly following the solar forcing. As a compromise, we decided to combine the 30 min average, with an average over the 15 canyon units ("ensemble average"). This 30 min ensemble average shows a small dispersive stress above the canopy, and local differences in velocity and temperature of about $0.1 m\,s^{-1}$ and $0.2 K$ compared to an 11 h average of a simulation with constant heat flux.
The focus of this study is on unstable atmospheric stratification and the simulations are done for a temperate mid-latitude climate (Boston, Massachusetts with latitude of 42.37), while the results can be expanded to various locations and time of the years using the characterization method further explained in Section 3. The simulation day is set to clear summer day (8th of July) and the forcing data is extracted from the representative Typical Meteorological Year (TMY3) file.
In a 3D urban environment with realistic heating, more than one urban surfaces is often heated (Figure 1). Solar noon at the simulation day is approximately at 1200 EDT. The convective heat flux at the roof surface is symmetric around solar noon, whereas Q_h at ground surfaces is higher in the afternoon hours due to the ground thermal storage (1). Accordingly, though solar flux received at east and west walls (leeward and windward, respectively) is symmetric around solar noon, due to the increased longwave radiation exchange between ground and wall surfaces in afternoon hours, Q_h at ground and wall surfaces exhibit larger value after 1200 EDT. Additionally, due to the sun path at the studied day, Q_h at the south wall is predominantly larger than the north wall with maximum heat flux difference occurring at 1330 EDT.

3. Characterizing momentum versus buoyancy forcing

Traditionally, the bulk Richardson number in the vertical direction Ri_v is used to indicate the atmospheric stability

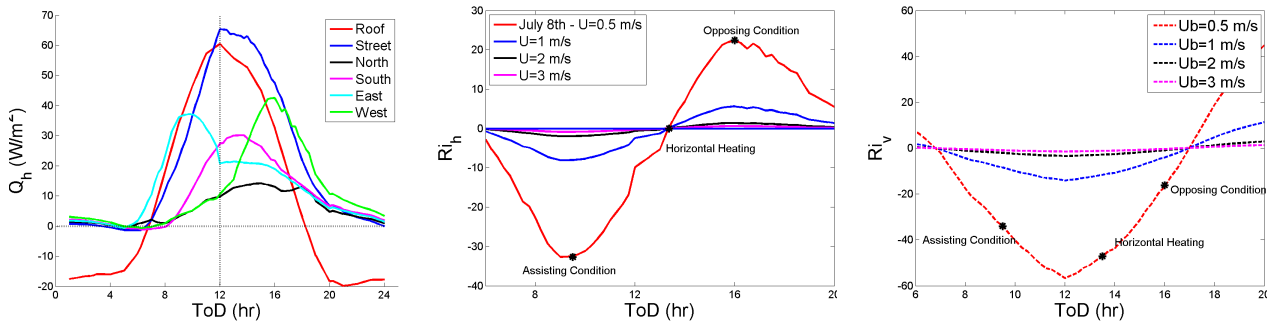

(a) (b) (c)

Figure 1: A) Horizontal Richardson number (Ri_h) and, b) vertical Richardson number (Ri_h) with ToD at different wind speed. c) Convective heat flux(Q_h) Q_h averaged at different urban facets for $U_b = 3\,\mathrm{ms}^-1$.

$$Ri_v = \frac{gH}{(U_b^2)} \frac{(\overline{T_H} - \overline{T_g})}{T_a} \ , \tag{1}$$

where $g = 9.81$ ms^{-1} is the gravitational acceleration, T_H is the air temperature at roof level, T_g is the temperature of the ground surface inside the building canyon, T_a is the inflow air temperature, and U_b is the bulk wind velocity in the streamwise direction. This methods alone neglects the horizontal temperature gradient, and fall short in comprehensive characterization of the flow. Therefore, horizontal Richardson number is also defined [11] to convey more information about the directionality of thermal forcing in relationship to the canyon vortex.

$$Ri_h = \frac{gH}{U_b^2} \frac{(\overline{T_L} - \overline{T_W})}{T_a} \frac{H}{W} \ , \tag{2}$$

where T_W and T_L are the averaged surface temperature on windward and leeward walls (here west and east), respectively. $\mathrm{Ri_h}$ indicates the effect of differential solar heating and also incorporates the effect of canyon aspect ratio H/W. The validity of this choice of non-dimensional numbers is demonstrated through simulations with different wind speed and surface radiative properties, but the same sets of Richardson numbers. Overall, similarity between two cases with same set of Richardson numbers is seen and the local normalized values in two cases are shown to be very close.

The average wind speed in simulation cases is varied from 0.5 to 8 $\mathrm{m\,s}^{-1}$ to span the weakly to strong unstable regimes. This setup results in a wide span of vertical and horizontal Richardson numbers (Figure 1) and according the analyses are performed for following conditions: a) assisting condition (0930 EDT) with maximum leeward heating occurring inside the canyon, i.e minimum Ri_h, and significant roof/ground heating, (Fig. 1), b) opposing condition (1600 EDT) when maximum windward heating occurs, i.e maximum Ri_h, combined with roof/ground heating and c) horizontal heating condition (1330 EDT) when both roof and ground surfaces are at maximum heating scenario with large Ri_v while west and east wall experience same average value of Q_h (Fig. 1), therefore $Ri_h = 0$. It is worth mentioning that when considering the realistic surface heating, wall and ground surfaces in the stream-wise canyons are also heated, therefore the thermal forcing in these conditions are more complex than cases previously studied by Cai [12].

4. Results

The analysis is structured as follows. First, the contour plots of flow, temperature and pollutant concentration are investigated at different locations in the stream/span-wise canyons. These detailed examinations further improve our understanding on the effects of three-dimensional heating orientation and strength

(quantified by sets of Richardson numbers) on pollutant distribution and the mechanisms involved in pollutant dispersion. An example of this analysis is shown in Section 4.1 (Figures 2 and 3), where the flow and concentration fields are evaluated together at different Richardson numbers.
Secondly, "Breathability" in urban environments is analyzed by studying the pollutant concentration distribution and exchange processes in the 3-D geometry. By adopting air quality concepts originally developed for indoor building environments, such as age of air, and Air and Pollutant Exchange Rate, outdoor ventilation is defined as a measure of city "breathability". An example of this analysis is described in Section 4.2.

4.1. Flow and dispersion fields

The contour plots of mean velocity magnitude superimposed by velocity vectors are shown in Figures 2 followed by the plots of dimensionless pollutant concentration in Figures 3. For brevity, only the results of $U_b = 0.5$ and $3\,\mathrm{ms}^{-1}$ are reported here and data are time-averaged over 1800s and ensemble averaged in the computational domain. The results are reported for the assisting, opposing, and horizontal heating conditions, with different Richardson numbers due to the variation of inlet bulk velocity.
Formation of the secondary vortex is only seen when the absolute value of the horizontal Richardson number is large ($U_b = 0.5\,ms^{-1}$), and the region of low velocity adjacent to the heated wall is enhanced in the opposing condition (Fig. 2). The intensity of the vortex decreases with the decrease in the magnitude of Ri_v (increase in U_b) and the region of low velocity extends deeper in the canyon. Nazarian and Kleissl 2015b showed that for the opposing condition ($Ri_h >0$), larger horizontal (streamwise) temperature gradient exists at the roof level, therefore a lower pressure gradient is observed inside the canyon compared to the assisting conditions ($Ri_h < 0$). This horizontal pressure gradient results in higher velocity at the roof level and higher kinetic energy entering the building canyon when $Ri_h >0$, as also shown in the Figure 2. On the contrary, assisting condition ($Ri_h < 0$) has the smallest intensity of vortex, and the difference is more significant for the larger Ri_v. At the horizontal heating condition ($Ri_h = 0$), the heat advected from the ground surface causes a larger temperature increase in the canyon than the convection from the roof, therefore increasing the strength of the vortex in the building canyon. It is worth mentioning that this behavior can be reversed when the more dominant roof heating decreases the vortex strength in the canyon [11].
Subsequently, the concentration is larger in the canyon at assisting compared to opposing conditions, and the horizontal heating condition has the lowest concentration due to the large vertical Richardson number, therefor enhanced mixing, in the absence of wall heating in the stream-wise canyon ($Ri_h = 0$). Dimensionless concentration increases with the decrease in vertical and horizontal Richardson numbers (larger U_b) since the flow approaches neutral stability conditions.

4.2. Air Exchange Rate

The concept of Air Exchange Rate in street canyon represents the volumetric air exchange (removal or entry) per unit time integrated over the ventilating faces of street canyons. Applying kinetic (mass) balance in the 3D street canyon, 3D-ACH is defined by sum of air exchange rates along the top and sides of the canyon as

$$<\mathrm{ACH_{top}}> = \frac{\int\int w_+ \mathrm{d}x\mathrm{d}y}{A_{top}} \;, <\mathrm{ACH_{side\pm}}> = \frac{\int\int v_\pm \mathrm{d}x\mathrm{d}z}{A_{side}} \;. \tag{3}$$

Here only velocities exiting the canyon are considered, i.e. w_+ are positive vertical velocities along the top plane and according to the orientation of the side plane, the sign of spanwise velocity (v) differs to represent air removal. A_{top} and A_{side} are the areas of top and side of the urban canyon. To analyze the relative effects of mean flow and fluctuations on air removal from the building canyon, ACH is calculated both using the velocity and local velocity fluctuations (e.g. $v' = v - \overline{v}$) and referred to as $\mathrm{ACH_w}$ and $\mathrm{ACH_{w'}}$, respectively. Figure 4 shows the time series of $\mathrm{ACH_w}$ and $\mathrm{ACH_{w'}}$ calculated for the simulation case with inlet bulk velocity of 3 $m\,s^{-1}$. The ventilating faces are identified as follows. In the span-wise building canyon, the vertical planes that bound the volume between the buildings are defined by their coordinate in span-wise (y) direction, where side +y and side -y are aligned with the north and south walls of the building, respectively. The horizontal surface at roof level in the span-wise and street-wise canyons are identified as building canyon and street canyon, "BC" and "SC", respectively.

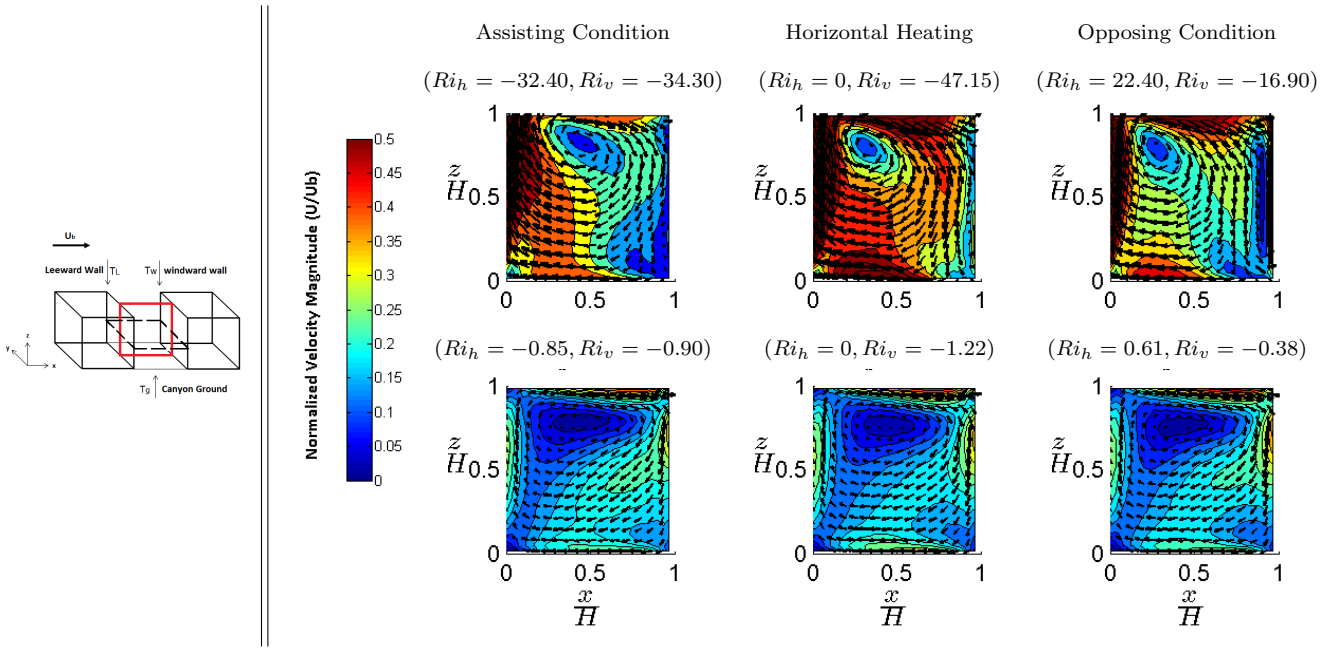

Figure 2: Contours of mean velocity magnitude normalized by bulk wind velocity, $\frac{\bar{U}}{U_b}$, overlaid by the mean velocity vector field at different conditions. Results are calculated at the vertical plane in the building canyon shown in red.

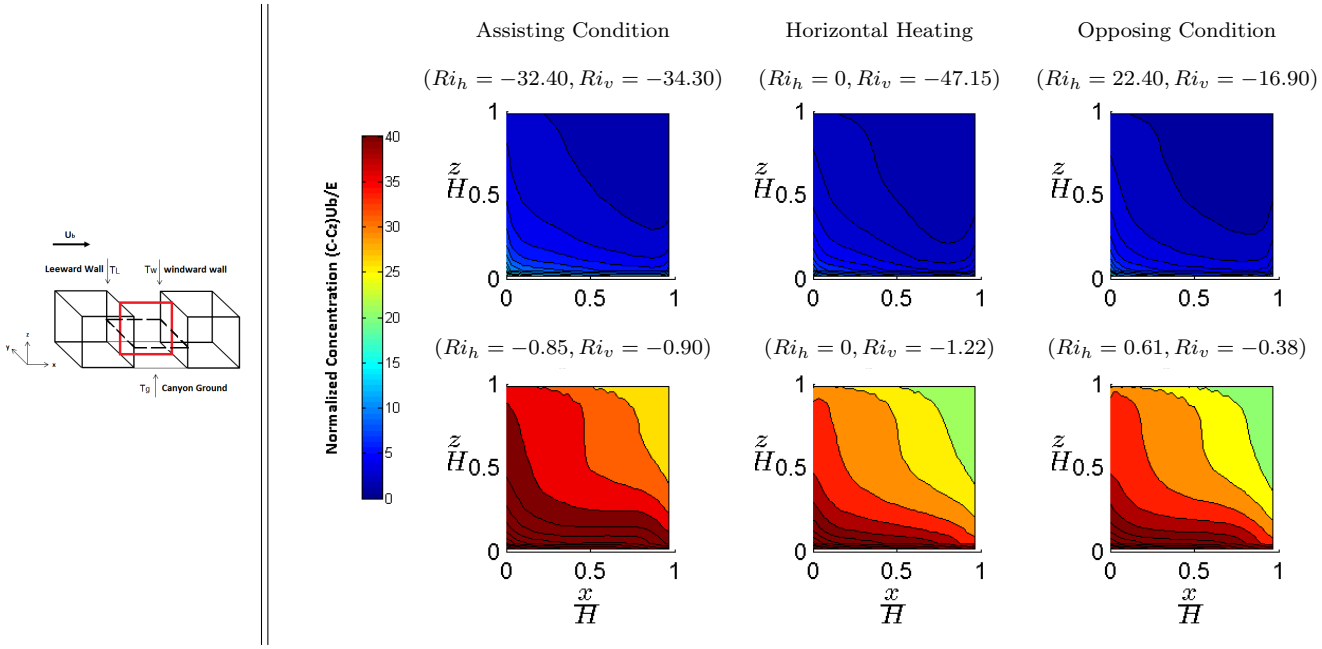

Figure 3: same as Fig 2 for dimensionless concentration $\frac{(\bar{C}-\bar{C}_z)}{E/U_b}$.

The ACH do not have a symmetrical behavior around solar noon throughout a day and are influenced by the sign of Ri_h. In the assisting conditions when Ri_h is negative and the Ri_v is also large, the ACH does not increase, presumably due to the effect of warm air advected in the canyon from the heated roof. The air exchanged from the horizontal surface at top of the building canyon (BC, spanwise canyon) is the largest

followed by south vertical ventilating face (side -y) and then north of the building canyon, with the horizontal surface at top of the street canyon (SC, stream-wise canyon) having the smallest value of ACH (Fig. 4). The difference between ACH_w and ACH'_w is significant at the top BC face and the south ventilating face (side -y), while at SC and north horizontal face (side +y) the velocity fluctuation has the main contribution to ACH. Pollutant Exchange Rate has a very similar patterns tp ACH (not shown) which demonstrates that the correlation between concentration and velocity does not change during the day. Therefore only by analyzing the flow field we can have an accurate calculation of pollutant exchange from the canyon level.

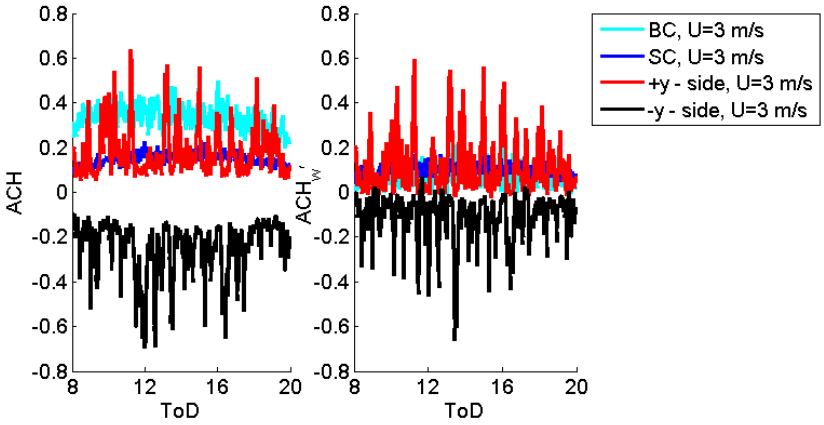

Figure 4: Comparison of instantaneous ACH calculated over all ventilating faces for $U_b = 3\,ms^{-1}$.

5. Conclusions

A three dimensional configuration of a compact urban environment is simulated with realistic surface heating and ground-level pollutant emission. The significance of considering realistic surface heating on the accurate analysis of pollutant dispersion is emphasized. Concentration distribution is shown to be correlated with horizontal and vertical Richardson numbers. Air Exchange Rate at street ventilating faces are analyzed and shown to have distinct characteristic according to the orientation and strength of the heated walls. Following this methodology, the study aims to further investigate the air quality and breathability in urban canopy.

References

[1] Y. Nakamura, T. Oke, Wind, temperature and stability conditions in an east-west oriented urban canyon, Atmospheric Environment (1967) 22 (12) (1988) 2691–2700.

[2] J.-F. Sini, S. Anquetin, P. G. Mestayer, Pollutant dispersion and thermal effects in urban street canyons, Atmospheric environment 30 (15) (1996) 2659–2677.

[3] S. Raasch, M. Schröter, Palm–a large-eddy simulation model performing on massively parallel computers, Meteorologische Zeitschrift 10 (5) (2001) 363–372.

[4] M. O. Letzel, M. Krane, S. Raasch, High resolution urban large-eddy simulation studies from street canyon to neighbourhood scale, Atmospheric Environment 42 (38) (2008) 8770–8784.

[5] N. Yaghoobian, J. Kleissl, An indoor–outdoor building energy simulator to study urban modification effects on building energy use–model description and validation, Energy and Buildings 54 (2012) 407–417.

[6] S.-B. Park, J.-J. Baik, S. Raasch, M. O. Letzel, A large-eddy simulation study of thermal effects on turbulent flow and dispersion in and above a street canyon, Journal of Applied Meteorology and Climatology 51 (5) (2012) 829–841.

[7] N. Yaghoobian, J. Kleissl, E. S. Krayenhoff, An improved three-dimensional simulation of the diurnally varying street-canyon flow, Boundary-Layer Meteorology 153 (2) (2014) 251–276.

[8] A. Kovar-Panskus, L. Moulinneuf, E. Savory, A. Abdelqari, J.-F. Sini, J.-M. Rosant, A. Robins, N. Toy, A wind tunnel investigation of the influence of solar-induced wall-heating on the flow regime within a simulated urban street canyon, Water, Air and Soil Pollution: Focus 2 (5-6) (2002) 555–571.

[9] O. Coceal, A. Dobre, T. G. Thomas, Unsteady dynamics and organized structures from dns over an idealized building canopy, International Journal of Climatology 27 (14) (2007) 1943–1953.

[10] M. Raupach, R. Shaw, Averaging procedures for flow within vegetation canopies, Boundary-Layer Meteorology 22 (1) (1982) 79–90.

[11] N. Nazarian, J. Kleissl, Effects of wall heating on flow characteristics in a street canyon, Building and Environment.

[12] X.-M. Cai, Effects of wall heating on flow characteristics in a street canyon, Boundary-layer meteorology 142 (3) (2012) 443–467.